

Normal Paper
 Student Paper
 Young Engineer Paper

TRICOM-1R Flight Dynamics Analysis; Angular Momentum Oscillation of Spinning Satellite in Highly Elliptical Orbit

Takayuki Hosonuma ¹, Takeshi Matsumoto ¹, Yoshihide Aoyanagi ¹, Toshihiro Obata ¹, Shinichi Nakasuka ¹

¹ *Department of Aeronautics and Astronautics, The University of Tokyo,
 7-3-1 Hongo, Bunkyo-ku, Tokyo, Japan*

Abstract

This paper reports the sinusoidal spin rate oscillation motion of a spinning-satellite in highly elliptical orbit experienced by TRICOM-1R. TRICOM-1R is a 3U CubeSat launched into highly elliptical orbit by the experimental small rocket. After separated from the rocket, the satellite spined around its minor axis with its spin rate of about 600 deg/sec as expected, and as the kinetic energy of the satellite decreased, the satellite became rotating around its major axis (flat-spin) with its spin rate of about 110 deg/sec. After the satellite went into the flat-spin motion, the spin rate of the satellite kept oscillating sinusoidally between 110 deg/sec and 170 deg/sec with its period of about 40 days. Telemetry analysis have been conducted to identify the cause of this spin rate oscillation. The results of the telemetry analysis and the numerical simulations suggest that the cause of the spin rate oscillation is the aerodynamic torques. In this paper, the details of the telemetry data and its analysis results are discussed.

Keywords: spinning-satellite, attitude dynamics, elliptical orbit, CubeSat, in-orbit data

Introduction

Overview of TRICOM-1R

TRICOM-1R is a 3U CubeSat for technological experiments developed by the University of Tokyo. The mission of the satellite is to demonstrate “Store and Forward” communication with very weak signal power, as well as to verify an autonomous on-board task planning function [1]. The satellite was launched into highly elliptical orbit by the experimental small sounding rocket SS-520 [2] in February 2018. TRICOM-1R had been operated from February 2018 to August 2018. After successfully finished its mission, the satellite re-entered to the earth’s atmosphere and was completely burned up in August 2018.

Fig. 1 shows the schematic overview of the TRICOM-1R satellite and Table 1 shows the mass property of the satellite. The size of the satellite is about 10 cm × 10 cm × 30 cm. The Z-axis of the body frame is parallel to the longer direction of the satellite, and the X-axis as well as the Y-axis of the body frame are orthogonal to the Z-axis. As a result, the Z-axis of the satellite is corresponding to the minor axis, i.e. the spin motion around the Z-axis is unstable in the case of the internal energy dissipation of the satellite is not negligible. Table 2 shows the components list of the attitude determination and control system (ADCS) implemented to TRICOM-1R satellite. Since the mission of the satellite is expected to be successfully achievable without any knowledge of the three-axis satellite attitude with respect to the inertial frame, the satellite is equipped with no attitude sensors for observing the three-axis attitude with respect to the inertial frame.

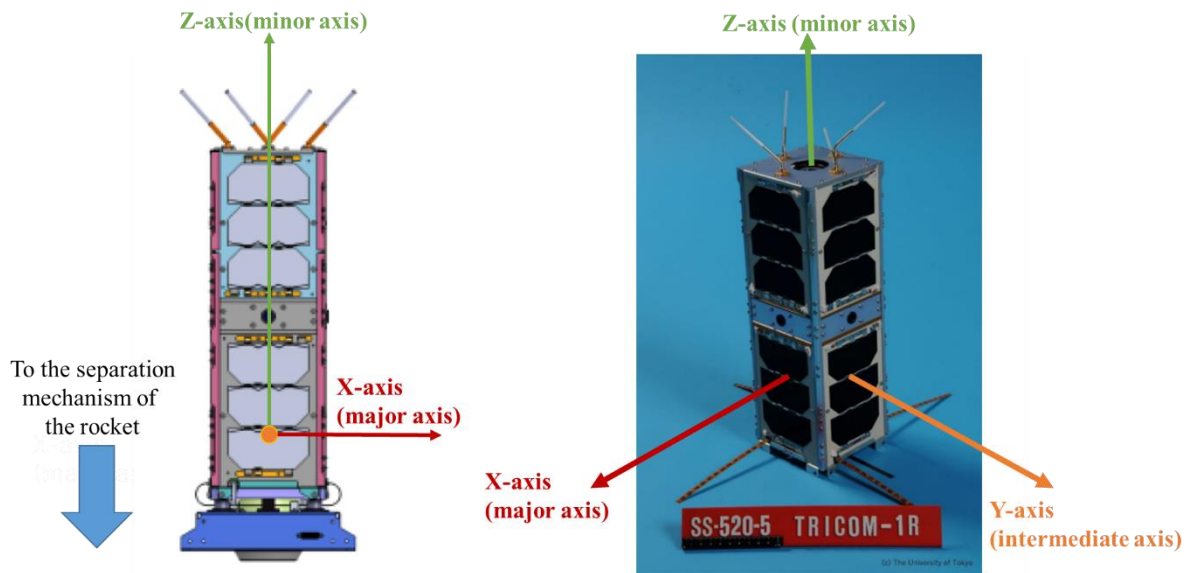


Fig. 1: Schematic Overview of TRICOM-1R

Table 1: Mass Property of TRICOM-1R

Property		Value	Units
size		116×116×346	[mm]
Mass		3.0	[kg]
Moment of Inertia	X	1.166E-02	[kgm ²]
	Y	1.162E-02	
	Z	2.722E-03	
centre-of-mass position with respect to centre-of-body chassis	X	-1.28	[mm]
	Y	-1.54	
	Z	-70.26	

Table 2: ADCS Components of TRICOM-1R

Attribute	components
Attitude Actuators	3-axis Magnetic Torquers
	1-axis Momentum Wheel
Attitude Sensors	3-axis Magnetic Sensor
	3-axis MEMS Gyro
	COTS GPSR

Sinusoidal Spin Rate Oscillation Motion

Fig. 2 shows the four months telemetry history of the satellite body rate. Fig. 3 shows the history of the angular momentum of the satellite in the satellite body frame. In Figs. 2 and 3, the horizontal axis of each graph corresponds to the elapsed days from the date the satellite launched. There is no unexpected behaviour in the history until 30 days passed from the launch. The initial (day 0 ~ day1) large body rate of 10 rad/sec (about 600 deg/sec) around the Z-axis (the minor axis) of the satellite is the tip-off rate. Due to the fact that the final stage of the rocket adopts spin-stabilized attitude control system but has no de-spin mechanisms [2], the satellite was separated from the rocket with large tip-off rate. During 12 days from the launch, the

satellite body rate around its minor axis gradually decreased to zero rad/sec while the body rate around the X-axis (the major axis) and the Y-axis (intermediate axis) are rapidly oscillating. This motion is similar to the spin transition phenomenon caused by the internal kinetic energy dissipation, which has been reported in many studies [3]~[5].

The spin rate oscillation motion focused in this paper begins after the spin transition (day 30~). After the spin transition (day 30~), the spin rate around the major axis and the intermediate axis of the satellite begin to oscillate sinusoidally. The period of this spin rate oscillation motion is about 40 days. The oscillation motion continues no less than three months. During this three-month term, all actuators of the satellite have been turned off, hence the cause of the oscillation motion is some form of the attitude disturbances.

In the following of this paper, the cause of this oscillation motion is studied. In the next section, the mechanism of the oscillation motion is discussed based on the analysis results of

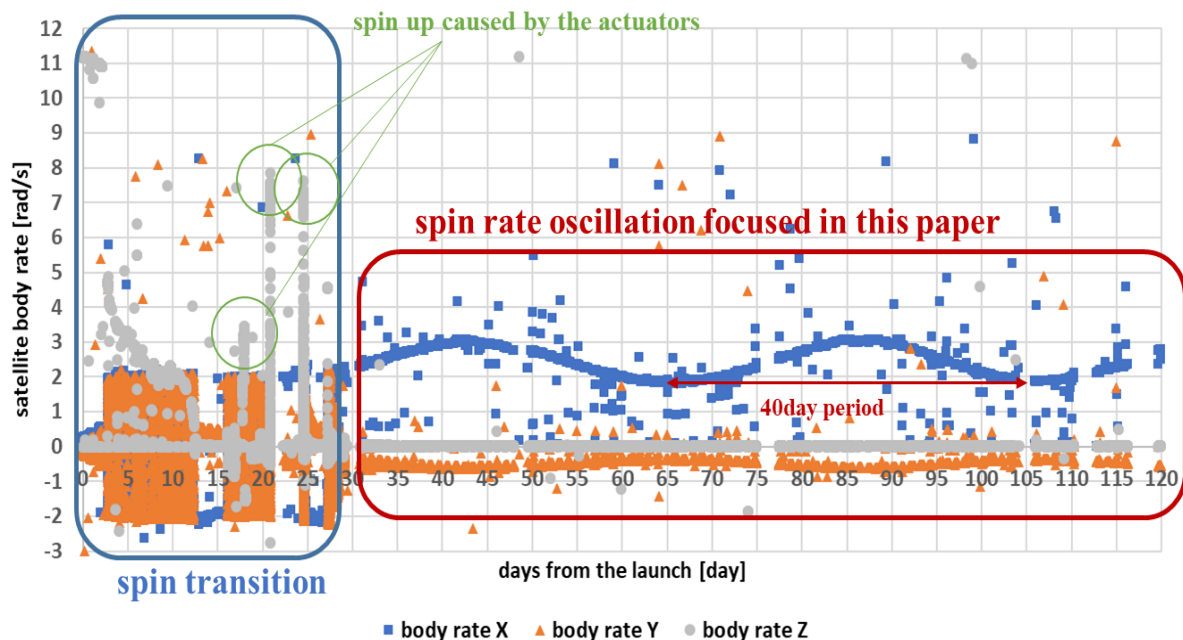


Fig. 2: Four months telemetry data history of the satellite body rate

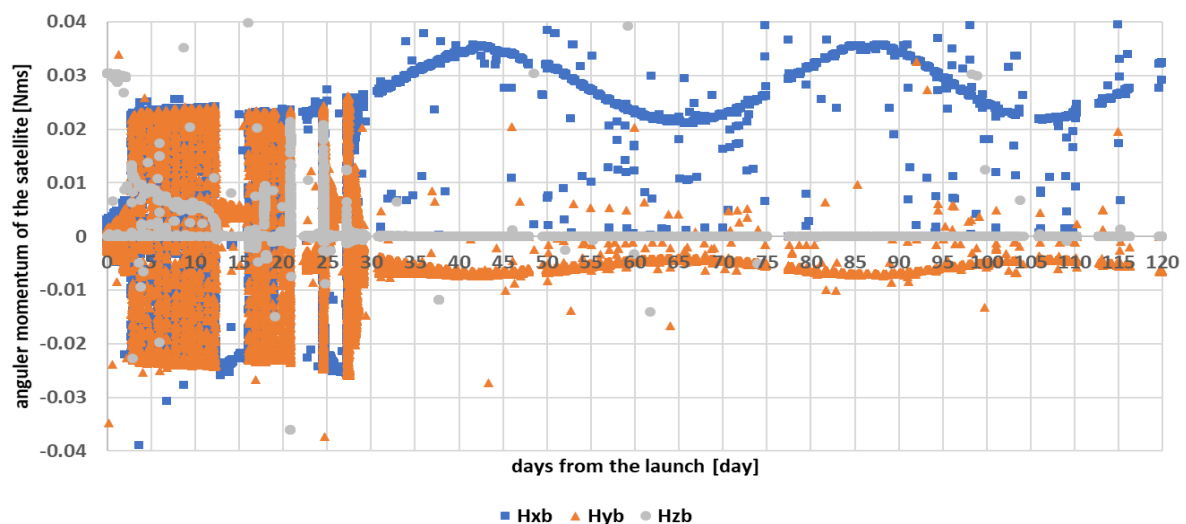


Fig. 3: Four months history of the angular momentum of the satellite in the body frame

the telemetry data sets. Then, after the next section, the discussed mechanism is verified with the numerical simulation. Finally, the results of the telemetry analysis and the numerical simulations are summarized as a conclusion.

Telemetry Analysis to Identify the Spin Rate Oscillation Mechanism

Telemetry Data Investigation

The fact that the spin rate oscillation motion has a period of tens of days suggests that the oscillation motion is related to the orbital dynamics of the satellite. Therefore, the analysis begins with comparing the period of the oscillation motion to the variation period of the satellite orbital elements. Fig. 4 shows the orbital elements extracted from NORAD two-line element (TLE) data files. Fig. 4 suggests that the rotation period of the argument of perigee (ω_p) of the

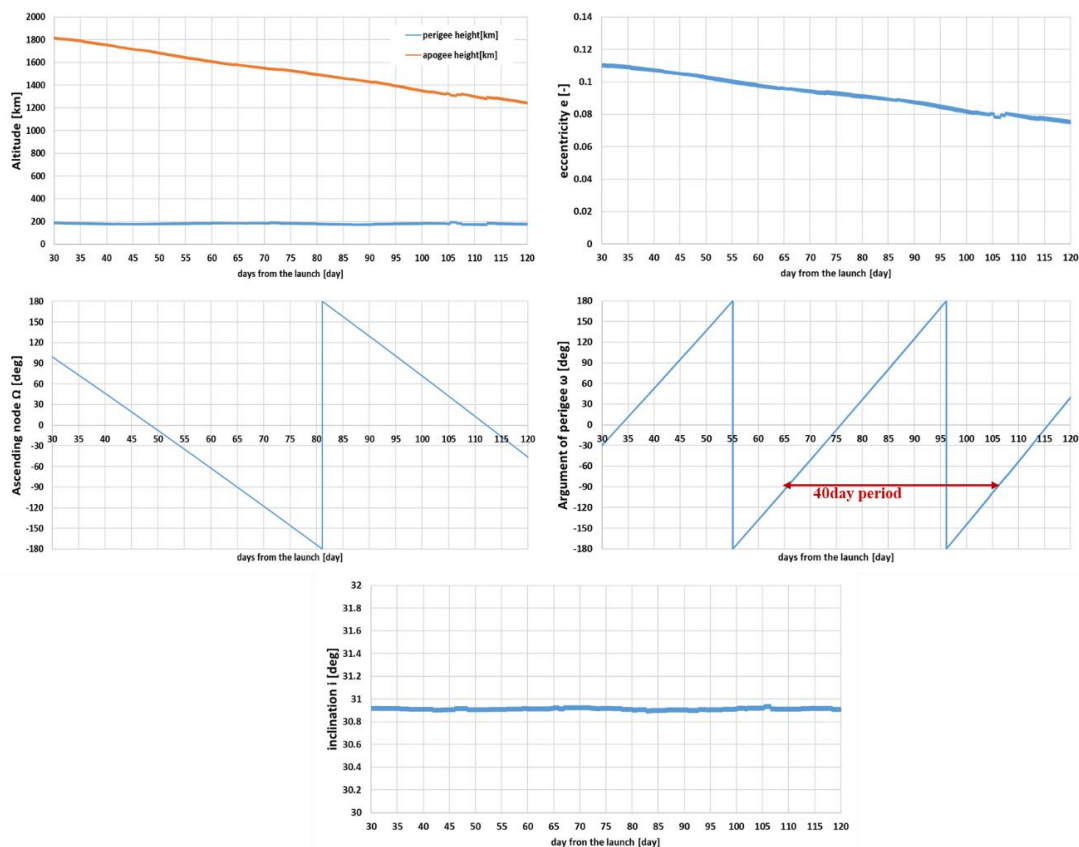


Fig. 4: Satellite orbital elements extracted from TLE data files

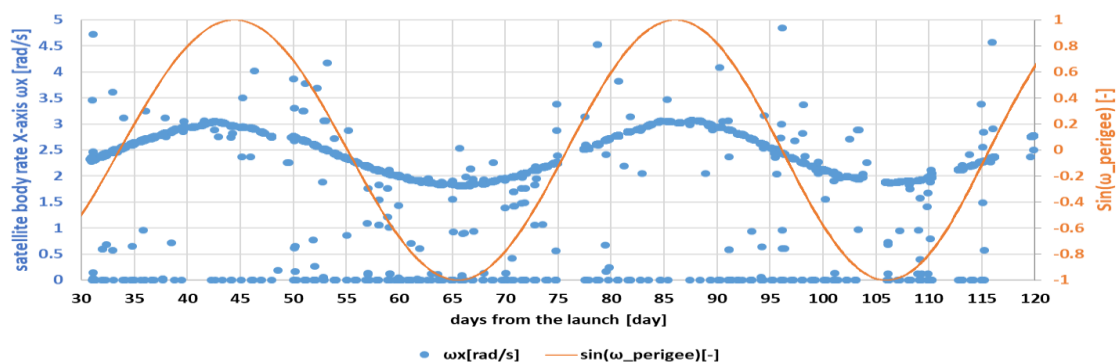


Fig. 5: Comparison between spin rate oscillation and perigee rotational motion ($\sin \omega_p$)

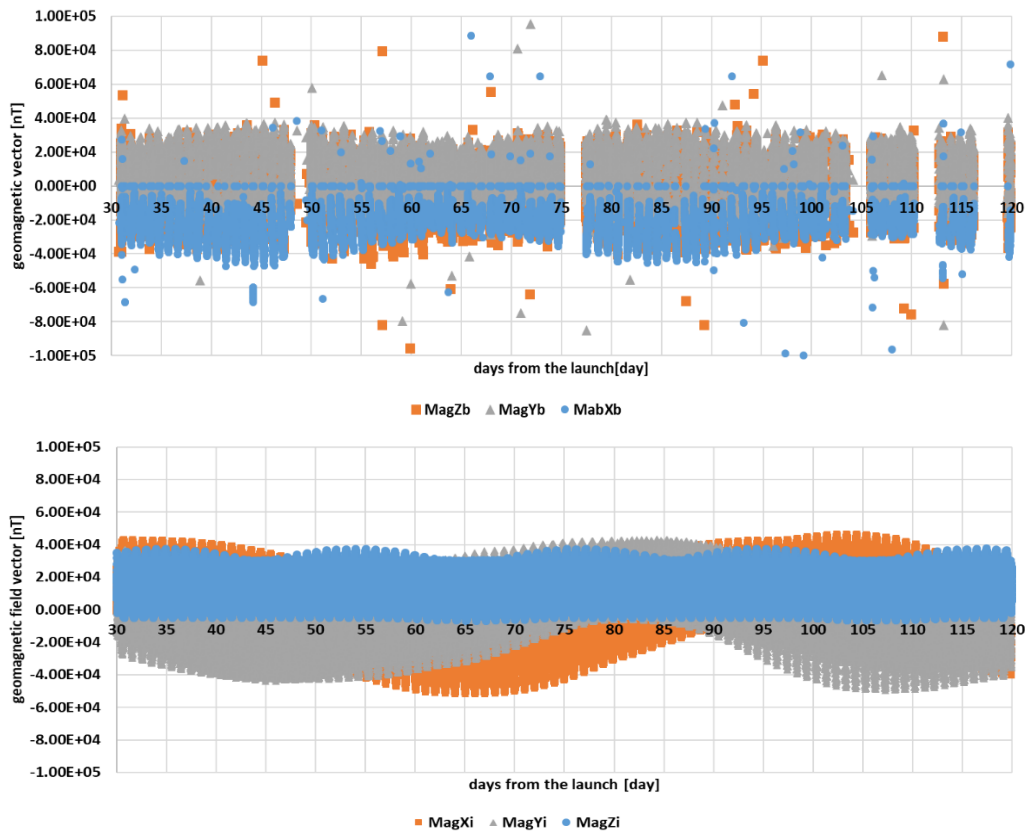


Fig. 6: Comparison between magnetic sensor data in body frame (top figure) and geomagnetic field in the inertial frame computed from IGRF (bottom figure)

satellite is almost equal to the period of the spin rate oscillation, while the variation period of the other orbital elements have no direct correlation with the period of the spin rate oscillation. In Fig. 5, $\sin \omega_p$ is compared to the satellite body rate around the major axis. From the figure, it is found that the spin rate oscillation motion is completely synchronised to the rotational motion of perigee direction of the satellite orbit. Additional information obtained from Fig. 4 is about the characteristic shape of the satellite orbit. The satellite is in highly elliptical orbit, whose apogee height is about 1800 km while its perigee height is about 200 km.

As a next step to estimate the cause of the spin rate oscillation motion, the X-axis direction of the satellite in inertial frame is estimated from the telemetry data. Because the satellite has no attitude sensor for observing the three-axis attitude of the satellite with respect to the inertial coordinate, the X-axis direction with respect to the inertial frame is estimated from the telemetry data of the magnetic sensor. In Fig. 6, the magnetic sensor data is compared to the geomagnetic field vector at the position of the satellite in the inertial frame, which is computed from IGRF combined with SGP4 for satellite position computation. The magnetic field vector component of the X-axis of the satellite (top figure, blue dots) is always negative, while the magnetic field vector component of the Z-axis in the inertial frame (bottom figure, blue dots) is almost always positive. This result suggests that the X-axis of the satellite is almost always aligned to the minus-Z (MZ) direction in the inertial frame.

Table 3 summarises the result of the telemetry analysis. 1) The spin rate transition motion showed in Fig. 2 suggests that the satellite has some kind of internal energy dissipation mechanism. 2) Figs. 4 and 5 suggests that the spin rate oscillation motion is completely synchronised to the rotational motion of perigee direction of the satellite orbit. 3) From Fig. 4, the satellite is in highly elliptical orbit, whose apogee height is about 1800 km while its perigee height is about 200 km. 4) The magnetic sensor data shown in Fig. 6 suggests that the X-axis

Table 3: Summary of the telemetry analysis results

1) The satellite has some kind of the internal energy dissipation mechanism
2) The spin rate oscillation motion is synchronised with the perigee rotation of the satellite orbit
3) The satellite orbit is highly elliptical orbit
4) The X-axis of the satellite body is almost fixed to the MZ direction of the inertial frame
5) The centre-of-mass position of the satellite is biased toward MZ direction of the satellite chassis

direction of the satellite body is aligned to the MZ-axis direction of the inertial frame. 5) As shown in Table 1, the centre-of-mass of the satellite is not adjusted to the geometrical centre of the satellite chassis. These results suggest that the aerodynamic torques causes the spin rate oscillation motion throughout the mechanism described in the following.

Spin Rate Oscillation Mechanism

From the telemetry analysis, it is found that the X-axis of the satellite body is almost always fixed to the MZ direction of the inertial frame. Therefore, the direction of the aerodynamic torques working around the Y-axis of the satellite body depends on the satellite position in the orbit. The aerodynamic torque works positive direction during the satellite is in its ascending orbital motion, while the aerodynamic torque works negative direction during the satellite is in its descending orbital motion, as described in Fig. 7. Fig. 8 shows the atmospheric density with respect to the satellite orbit computed from NRLMSISE atmospheric model. The atmospheric density at the perigee altitude of the satellite orbit (200 km) is more than $1e6$ times larger than the density at the apogee altitude of the satellite orbit (1800 km). Thus, the aerodynamic torque imposed to the satellite during the satellite is around the perigee is so large that the aerodynamic torque imposed to the satellite during the satellite is in the other position of its orbit is negligible. From these results, it could be concluded that the aerodynamic torque around the Y-axis of the satellite body oscillates sinusoidally with the same period as the rotational motion of the perigee direction of the satellite orbit.

As the aerodynamic torques works around the Y-axis of the satellite body frame, the angular momentum of the satellite and the kinetic energy of the satellite changes. As a result, the satellite starts nutation motion. And then, due to the internal energy dissipation, the nutation motion settled to the spin motion around the major axis of the satellite body. Throughout this process, the aerodynamic torques which works around the Y-axis of the satellite body causes the variational change of the satellite body rate around the X-axis.

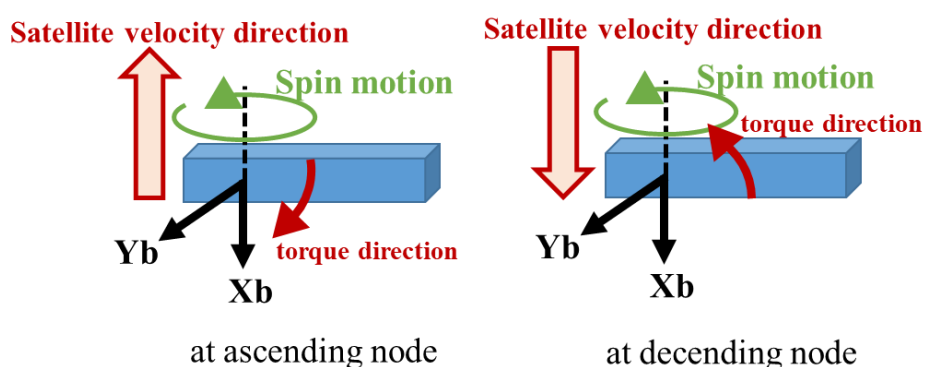


Fig. 7: Direction of the aerodynamic torques with respect to the satellite orbital velocity

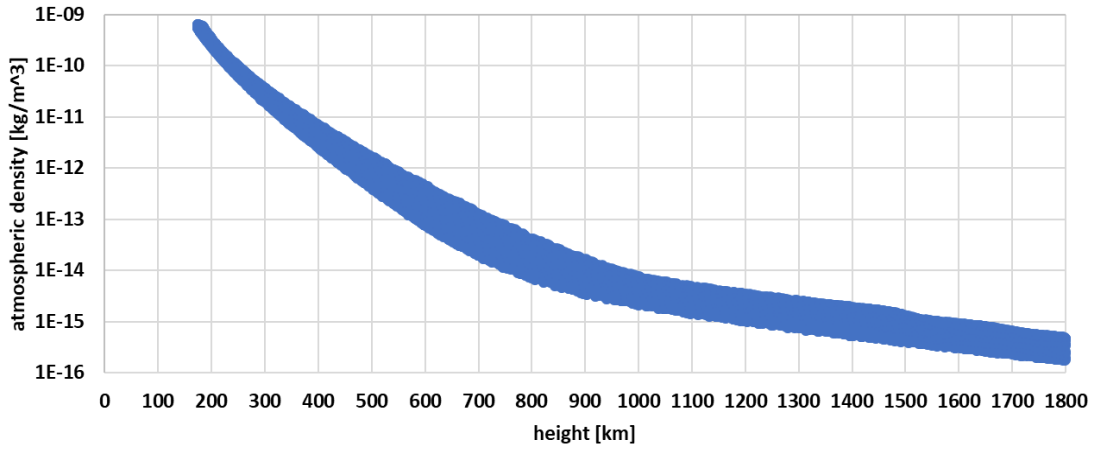


Fig. 8: Semi-logarithmic plot of atmospheric density with respect to the satellite altitude

The mechanism of the spin rate oscillation discussed above is summarised as follows. 1) Around the perigee of the orbit, the large aerodynamic torques works around the Y-axis of the satellite, which causes nutation motion of the satellite. 2) Due to the internal energy dissipation, the nutation motion of the satellite is settled to the spin motion around the X-axis, which is the major axis of the satellite. Throughout this process, the aerodynamic torques imposed around the Y-axis of the satellite causes variation of the body rate around the X-axis of the body. 3) As the perigee of the satellite orbit rotates, the direction of the aerodynamic torques changes sinusoidally. 4) Throughout these processes, the X-axis of the satellite sinusoidally oscillates.

Verification of the Oscillation Mechanism with Numerical Simulations

Simulation Models

To verify the mechanism described above, the numerical simulation has been conducted. In the simulation, for the purpose of considering internal energy dissipation effects, the satellite is modelled as a rigid body with a spherical slug surrounded by a viscous layer. In this case, the rotational equation of motion of the satellite is written as following [4], [5],

$$(I_{px} - J)\dot{\omega}_{px} - (I_{py} - I_{pz})\omega_{py}\omega_{pz} - \delta\sigma_x = T_{px} \quad (1)$$

$$(I_{py} - J)\dot{\omega}_{py} + (I_{px} - I_{pz})\omega_{px}\omega_{pz} - \delta\sigma_y = T_{py} \quad (2)$$

$$(I_{pz} - J)\dot{\omega}_{pz} - (I_{px} - I_{py})\omega_{px}\omega_{py} - \delta\sigma_z = T_{pz} \quad (3)$$

$$\dot{\sigma}_x + \dot{\omega}_{px} + \left(\frac{\delta}{J}\right)\sigma_x + \omega_{py}\sigma_z - \omega_{pz}\sigma_y = 0 \quad (4)$$

$$\dot{\sigma}_y + \dot{\omega}_{py} + \left(\frac{\delta}{J}\right)\sigma_y + \omega_{pz}\sigma_x - \omega_{px}\sigma_z = 0 \quad (5)$$

$$\dot{\sigma}_z + \dot{\omega}_{pz} + \left(\frac{\delta}{J}\right)\sigma_z + \omega_{px}\sigma_y - \omega_{py}\sigma_x = 0 \quad (6)$$

where, I_{px}, I_{py}, I_{pz} means the principle moment of inertia of the satellite, J means the inertia of the spherical slug, δ means viscosity of the viscous layer, $\omega_{px}, \omega_{py}, \omega_{pz}$ means angular velocity of the satellite in the coordinate of the principle axis of inertia, T_{px}, T_{py}, T_{pz} means attitude disturbance torques in the coordinate of the principle axis of inertia. Because the satellite has

the product of inertia, $\omega_{px}, \omega_{py}, \omega_{pz}$ are not equal to the satellite body rate $\omega_x, \omega_y, \omega_z$. The relationship between $\omega_{px}, \omega_{py}, \omega_{pz}$ and $\omega_x, \omega_y, \omega_z$ is written as following,

$$RI_b R^{-1} = I_p \quad (7)$$

$$RT_b = T_p \quad (8)$$

$$R\omega_b = \omega_p \quad (9)$$

where, $I_p = \text{diag}\{I_{px}, I_{py}, I_{pz}\}$, $T_p = [T_{px}, T_{py}, T_{pz}]^t$, $\omega_p = [\omega_{px}, \omega_{py}, \omega_{pz}]^t$, $\omega_b = [\omega_x, \omega_y, \omega_z]^t$. I_b means moment of inertia tensor of the satellite in the satellite body frame. T_b means the attitude disturbance torques in the satellite body frame. R means the coordinate transformation matrix. The parameters δ , J , and R are determined so that the simulation result of the spin transition motion agrees to the spin transition motion experienced in the orbit.

In the simulation, the aerodynamic torques is modelled by reference to [6], [7], as following,

$$T_{aero} = \sum_i \rho V_R^2 A_i H(\cos \alpha_i) [\sigma_t (\mathbf{r}_i \times \overline{\mathbf{V}}_R) + \{\sigma_n S + (2 - \sigma_n - \sigma_t) H(\cos \alpha_i)\} (\mathbf{r}_i \times \overline{\mathbf{n}}_i)] \quad (10)$$

$$H(\cos \alpha_i) = \begin{cases} 1 & (\text{if } \cos \alpha_i \geq 0) \\ 0 & (\text{otherwise}) \end{cases} \quad (11)$$

where, ρ means atmospheric density. V_R means relative velocity of the atmosphere with respect to the satellite. A_i means surface area of i-th satellite panel. $\cos \alpha_i$ means cosine of angle between unit atmospheric velocity vector $\overline{\mathbf{V}}_R$ and the normal unit vector of i-th satellite panel $\overline{\mathbf{n}}_i$. σ_t and σ_n means the tangential accommodation coefficients and the normal accommodation coefficients, respectively. \mathbf{r}_i means the arm vector from the centre-of-mass to the centre of i-th satellite panel. S means ratio of molecular exit velocity to atmospheric velocity.

In the simulation, the satellite orbit is computed from SGP4 using NORAD TLE data files. The initial date of the simulation scenario is chosen to 30 days after the launch date of the satellite. The initial body rate of the satellite is adjusted to the body rate observed in orbit at 30 days after the launch, and the initial satellite attitude is adjusted so that the X-axis of the satellite body is aligned to the MZ direction of the inertial frame.

Simulation Results

Fig. 9 compares the simulation result of the satellite body rate to the in-orbit result of the satellite body rate. It can be seen in Fig. 9 that the oscillation period and amplitude of satellite body rate in the simulation result almost agrees to the oscillation period of the satellite body rate in the telemetry data. In Fig. 10, the output history of the X-axis components of the magnetic sensor during the simulation scenario is compared to the in-orbit data of the magnetic sensor of the satellite. In both of the simulation result and the in-orbit data, the X-axis components of the magnetic sensor output is biased to negative value. These results indicate that the spin rate oscillation motion experienced by TRICOM-1R is reproduced in the simulation scenario.

The top figure in Fig. 11 shows the history of the Y-axis components of the computed aerodynamic torques during the simulation scenario. From this figure, as expected from the rate oscillation mechanism described in the previous section, it can be seen that the Y-axis components of aerodynamic torque oscillates with 40 days period, which is equal to the period of the perigee rotation. The bottom figure in Fig. 11 shows the Y-axis components of the computed aerodynamic torques during initial 60000 sec period of the simulation scenario. From

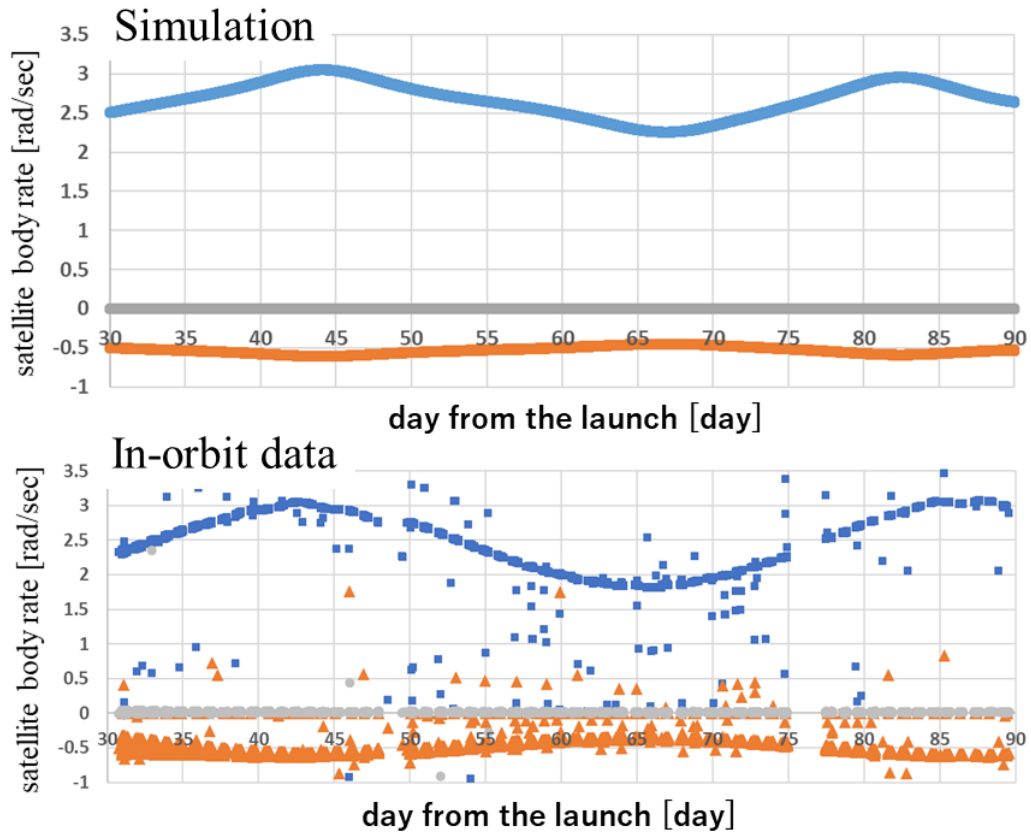


Fig. 9: Comparison between simulation result and in-orbit data focused on the body rate

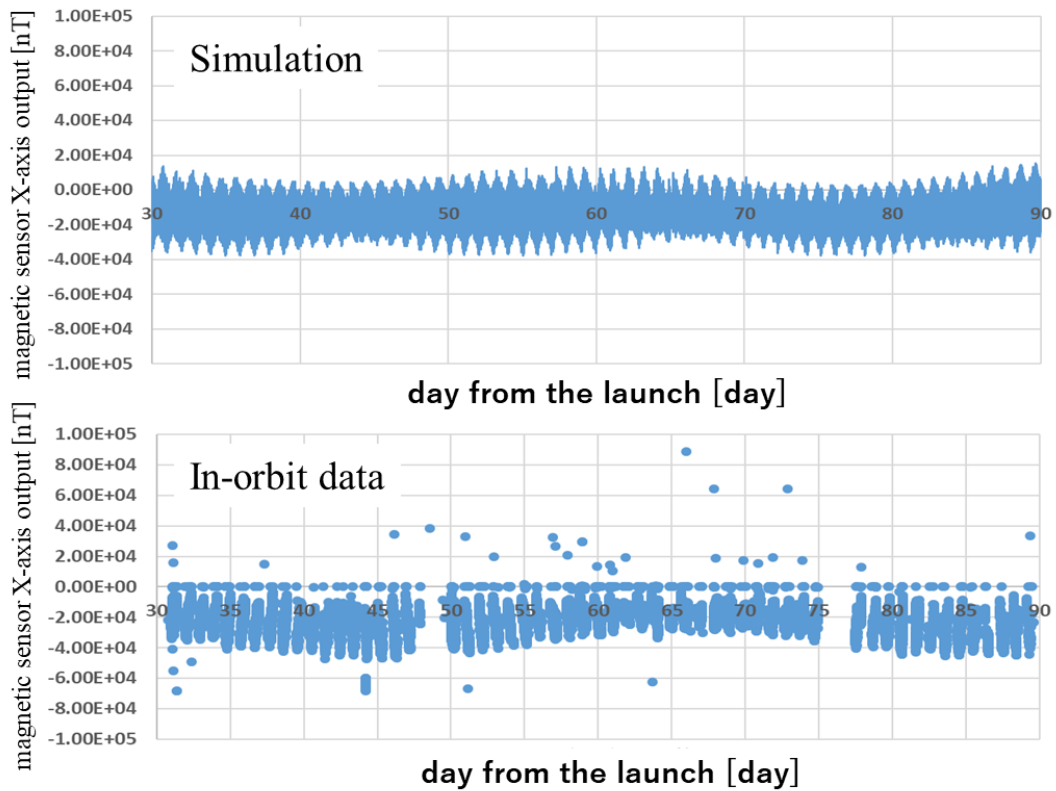


Fig. 10: Comparison between simulation result and in-orbit data focused on the magnetic sensor output

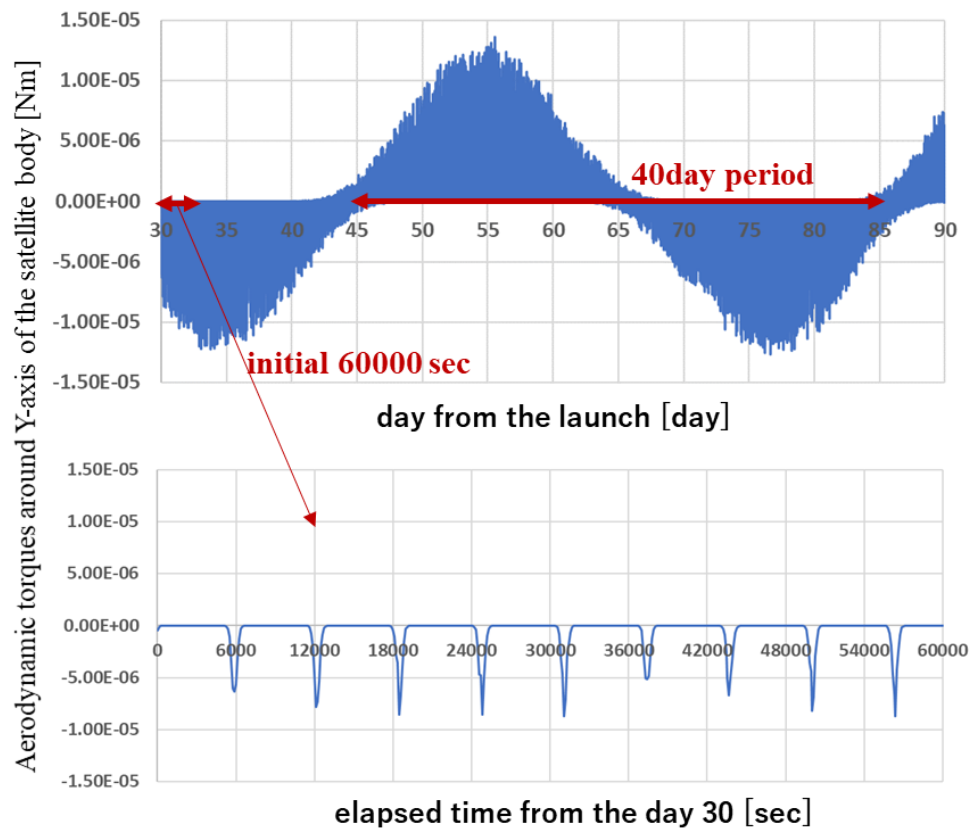


Fig. 11: simulation result of aerodynamic torques during the simulation scenario (top figure) and its initial 60000 sec data (bottom figure)

this figure, it can be seen that comparing to the magnitude of the aerodynamic torques at the several peak timings, the magnitude of the torques during the rest timing is much small. This results agrees to the previous expectation that the aerodynamic torque imposed to the satellite during the satellite is around the perigee is so large that the aerodynamic torque imposed to the satellite during the satellite is in the other position of its orbit is negligible.

From these results, it could be concluded that the spin rate oscillation motion in orbit is reproduced in the simulation scenario, and in the simulation scenario, the behaviour of the aerodynamic torques agrees to the behaviour expected from the oscillation mechanism described in the previous section. Thus, these simulation results support the validity of the spin rate oscillation mechanism described in the previous section.

Conclusion

This paper reports the sinusoidal spin rate oscillation motion of a spinning-satellite in highly elliptical orbit experienced by TRICOM-1R. From the TRICOM-1R telemetry data, it is found that during the flat-spin motion of the satellite, the spin rate of the satellite kept oscillating sinusoidally between 110 deg/sec and 170 deg/sec with its period of about 40 days. The oscillation motion continues no less than three months. During this three-month term, all actuators of the satellite have been turned off, hence the cause of the oscillation motion is some form of the attitude disturbances.

Telemetry analysis has been conducted to identify the cause of the spin rate oscillation. The results of the telemetry analysis suggest that the aerodynamic torques causes the spin rate oscillation motion throughout the mechanism as following. 1) Around the perigee of the orbit, the large aerodynamic torques works around the Y-axis of the satellite, which causes nutation motion of the satellite. 2) Due to the internal energy dissipation, the nutation motion of the

satellite is settled to the spin motion around the X-axis, which is the major axis of the satellite. Throughout this process, the aerodynamic torques imposed around the Y-axis of the satellite causes variation of the X-axis body rate. 3) As the perigee of the satellite orbit rotates, the direction of the aerodynamic torques changes sinusoidally. 4) Throughout these processes, the X-axis of the satellite sinusoidally oscillates.

To verify the mechanism described above, the numerical simulation has been conducted. The simulated satellite body rate and the magnetic sensor output agrees well to the in-orbit history of the satellite body rate and the magnetic sensor output. In addition, the aerodynamic torques computed in the simulation scenario sinusoidally oscillates with 40 days period, which is equal to the period of the spin rate oscillation motion.

From these results, it could be concluded that the spin rate oscillation motion experienced by TRICOM-1R is caused by the sinusoidal variation of the aerodynamic torques triggered by the rotational motion of the perigee direction of the satellite orbit.

References

1. Obata, T., Nakasuka, S., Aoyanagi, Y., Mastumoto, T., and Shirasaka, S., “The Goal-oriented Robust Operations and Their Demonstration on Orbit”, *Proceedings of SpaceOps Conferences 2018*, Marseille, France, 2018
2. Inatani, Y., Ohtsuka, H., “SS-520 Nano satellite launcher and its flight result”, *Proceedings of 32nd Annual AIAA/USU Conference on Small Satellite 2018*, Logan, Utah, USA, 2018
3. Likins, P.W., “Effects of Energy Dissipation on the Free Body Motions of Spacecraft”, *NASA Jet Propulsion Laboratory Technical Report*, No.32-860, 1966
4. Rahn, C.D., Barba, P.M., “Reorientation Maneuver for Spinning Spacecraft”, *Journal of Guidance, Control, and Dynamics*, vol. 14, No. 4, 1991, pp. 724-728
5. Livneh, R., Wie, B., “Asymmetric Body Spinning Motion with Energy Dissipation and Constant Body-Fixed Torques”, *Journal of Guidance, Control, and Dynamics*, vol. 22, No. 2, 1999, pp. 322-328
6. Steyn, W.H., Kearney, M., “An Attitude Control System for ZA-AeroSat subject to significant Aerodynamic Disturbances”, *Proceedings of the 19th World Congress The International Federation of Automatic Control*, Cape Town, South Africa, 2014, pp. 7929-7934
7. Gargasz, M.L., “Optimal spacecraft attitude control using aerodynamic torques”, *Thesis for Master degree*, Air Force Institute of Technology, USA, 2007